RESEARCH ARTICLE

Blood Science

OPEN

Exosome miRNAs profiling in serum and prognostic evaluation in patients with multiple myeloma

Teng Fang[a,b], Hao Sun[a,b], Xiyue Sun[a,b], Yi He[a], Peixia Tang[c], Lixin Gong[a,b], Zhen Yu[a,b], Lanting Liu[a,b], Shiyi Xie[a,b], Tingyu Wang[a], Zhenshu Xu[c], Shuhua Yi[a], Gang An[a], Yan Xu[a], Guoqing Zhu[a], Lugui Qiu[a,b,d,*], Mu Hao[a,b,*]

[a]State Key Laboratory of Experimental Hematology, National Clinical Research Center for Blood Diseases, Haihe Laboratory of Cell Ecosystem, Institute of Hematology & Blood Diseases Hospital, Chinese Academy of Medical Sciences & Peking Union Medical College, Tianjin 300020, China; [b]Tianjin Institutes of Health Science, Tianjin 301600, China; [c]Hematology Department, Fujian Medical University Union Hospital, Fujian Institute of Hematology, Fuzhou 350001, China; [d]Gobroad Healthcare Group, Beijing 100072, China

Abstract

MicroRNAs (MiRNAs) carried by exosomes play pivotal roles in the crosstalk between cell components in the tumor microenvironment. Our study aimed at identifying the expression profile of exosomal miRNAs (exo-miRNAs) in the serum of multiple myeloma (MM) patients and investigating the regulation networks and their potential functions by integrated bioinformatics analysis. Exosomes in serum from 19 newly diagnosed MM patients and 9 healthy donors were isolated and the miRNA profile was investigated by small RNA sequencing. Differential expression of exo-miRNAs was calculated and target genes of miRNAs were predicted. CytoHubba was applied to identify the hub miRNAs and core target genes. The LASSO Cox regression model was used to develop the prognostic model, and the ESTIMATE immune score was calculated to investigate the correlation between the model and immune status in MM patients. The top six hub differentially expressed serum exo-miRNAs were identified. 513 target genes of the six hub exo-miRNAs were confirmed to be differentially expressed in MM cells in the Zhan Myeloma microarray dataset. Functional enrichment analysis indicated that these target genes were mainly involved in mRNA splicing, cellular response to stress, and deubiquitination. 13 core exo-miRNA target genes were applied to create a novel prognostic signature to provide risk stratification for MM patients, which is associated with the immune microenvironment of MM patients. Our study comprehensively investigated the exo-miRNA profiles in MM patients. A novel prognostic signature was constructed to facilitate the risk stratification of MM patients with distinct outcomes.

Key Words: Bioinformatics analysis, Exosome, MicroRNA, Multiple myeloma, Prognosis evaluation

** Address correspondence: Dr. Mu Hao and Dr. Lugui Qiu, State Key Laboratory of Experimental Hematology, National Clinical Research Center for Blood Diseases, Institute of Hematology & Blood Diseases Hospital, No. 288 Nanjing Road, Tianjin 300020, China. E-mail address: haomu@ihcams.ac.cn (M. Hao); qiulg@ihcams.ac.cn (L. Qiu).*

Conflict of interest: The authors declare that they have no conflict of interest.

T.F. and H.S. contributed equally.

This work was supported by the National Natural Science Foundation of China (82170194, 81920108006, 82270175), and the CAMS Innovation Fund for Medical Sciences (CIFMS 2021-I2M-1-040, CIFMS 2022-I2M-022).

This study was approved by the Institutional Ethics Review Boards with approval number KT2020010-EC-2 from the Institute of Hematology and Blood Diseases Hospital, Chinese Academy of Medical Sciences, Tianjin. Written informed consent was obtained from patients and healthy donors before sample collection.For original data and code, please contact the corresponding author, haomu@ihcams.ac.cn.

Blood Science (2023) 5, 196–208

Received December 14, 2022; Accepted April 18, 2023.

http://dx.doi.org/10.1097/BS9.0000000000000160

1. INTRODUCTION

Multiple myeloma (MM) is an incurable hematological malignancy characterized by the clonal expansion of malignant plasma cells in the bone marrow.[1] Tight crosstalk between the bone marrow microenvironment and MM cells plays a pivotal role in the development and progression of MM.[2–4] Our previous studies showed that exosomes released by MM cells could be taken up by surrounding cells, especially immune cells, promoting MM cell survival, drug resistance, and immune escape.[3,4]

Exosomes are small extracellular vesicles (EVs) with a diameter of 30 to 100 nm, which are produced and actively released by living cells. More exosomes are released by malignant compared with normal cells, suggesting that exosomes play pivotal roles in the process of signaling transfer between malignant and nonmalignant cells, thereby facilitating tumor progression.[5] Exosomes act as intercellular mediators by carrying and releasing active contents, including noncoding RNA (ncRNA), DNA, proteins and lipids.[6,7] MicroRNA (miRNA) is a type of single-stranded noncoding RNA composed of 20 to 24 nucleotides (nt) that in different ways can regulate gene expression at the posttranscriptional level.[8,9] It has been shown that exosomal miRNA (exo-miRNA) profiles were diverse between MM cells and normal counterparts and could be used to predict survival in myeloma patients.[10,11] Of note, miRNAs carried by exosomes are important mediators of crosstalk and signal to transfer between the bone marrow

microenvironment and myeloma cells.[12,13] MiRNAs secreted by exosomes are associated with various alterations in the MM microenvironment including angiogenesis, activation of osteolysis, immune system modulation, and induction of drug resistance.[14] However, the comprehensive functional network and molecular mechanisms of miRNAs and their target genes in myeloma progression and poor patient prognosis remain poorly understood.

In this study, the serum exo-miRNA expression profiles in newly diagnosed (ND) MM patients were investigated. The regulatory network between miRNA and mRNA was further analyzed, and the hub miRNAs and key mRNAs were clarified. The potential underlying mechanism of exo-miRNAs and their target genes involved in MM pathogenesis was also investigated. A novel prognostic model based on a 13-core-genes signature was constructed to further facilitate predicting the clinical prognosis of MM, which was also correlated with the immune suppressive microenvironment. Altogether, our study furthers our understanding of the exo-miRNA and mRNA functional network, and the overwhelmingly complex interaction between MM cells and the bone marrow microenvironment, which could provide novel promising targets for therapeutic strategies.

2. MATERIALS AND METHODS

2.1. Sample collection and ethics statement

Peripheral blood samples were collected from 9 healthy donors and 19 NDMM patients. Following routine venipuncture procedures, peripheral blood samples were collected in procoagulant tubes, centrifuged at 3500 r/min for 10 minutes at 4°C, and the supernatant serum was stored at −80°C until testing.

2.2. Exosome isolation

Exosomes were isolated by size exclusion chromatography. Briefly, 1 mL of 0.8 μm-filtered serum was diluted 1.5-fold with phosphate-buffered saline and further purified using Exosupur columns (Echobiotech, China) following the manufacturer's instructions. Fractions were concentrated to 200 μL by 100 kDa molecular weight cutoff Amicon Ultra spin filters (Merck, Germany). The obtained exosome samples were observed by transmission electron microscopy, the particle size distribution was measured by nanoparticle tracking analysis using ZetaView PMX 110 (Particle Metrix, Meerbusch, Germany), and their concentration was determined. The exosomes were also identified by western blot analysis using rabbit polyclonal antibody CD63 (sc-5275, Santa Cruz, CA, USA), CD9 (60232-I-Ig, Proteintech, Rosemont, IL), HSP90 (60318-I-Ig, Proteintech, Rosemont, IL), Alix (sc-53540, Santa Cruz, CA, USA), TSG101 (sc-13611, Santa Cruz, California) and calnexin (10427-2-AP, Promega, Madison, Wisconsin). The proteins were visualized on the Tanon4600 Automatic chemiluminescence image analysis system (Tanon, Shanghai, China).

2.3. RNA extraction, small RNA library construction, and sequencing

Total RNA was extracted and purified from serum exosomes using miRNeasy® Mini kit (Qiagen, Frederick, Maryland, Cat. No. 217004) according to the kit instructions. A total amount of 0.5 μg RNA per sample was used as input material for the RNA sample preparations. Sequencing libraries were generated using QIAseq miRNA Library Kit (Qiagen) following the manufacturer's recommendations and index codes were added to attribute sequences to each sample. Library quality was assessed on the Agilent Bioanalyzer 2100 and qPCR. The clustering of the index-coded samples was performed on the acBot Cluster Generation System using TruSeq PE Cluster Kitv3-cBot-HS (Illumina, San Diego, California) according to the manufacturer's instructions. After cluster generation, the library preparations were sequenced on an Illumina Hiseq 2500 platform, and single-end 50 nt reads were generated (Beijing Biomarker Technologies Co., Ltd, Beijing, China).

2.4. RNA-seq data processing

Raw data of fastq format were first processed through in-house Perl scripts. In this step, clean data were obtained from raw data by removing reads containing adapters, reads containing ploy-N and low-quality reads. Reads were also trimmed and cleaned by removing the sequences smaller than 18 nt or longer than 30 nt. Using Bowtie[15] software, the clean reads were aligned with the Silva database, GtRNAdb database, Rfam database, and Repbase database, respectively, to filter ribosomal RNA (rRNA), transfer RNA (tRNA), small nuclear RNA (snRNA), ncRNAs such as small nucleolar RNA (snoRNA) and repeated sequences. The remaining reads were used to detect known miRNAs by aligning with Human Genome (GRCh38) and known miRNAs from miRbase (release 22). The miRDeep2[16] was applied to predict the new miRNA using the Bayesian model.

2.5. Quantification and differential expression analysis of miRNAs

The read count for each miRNA was obtained from the mapping results, and FPKM was computed. Differential expression of identified miRNAs from miRbase was calculated using the edgeR package[17] (version 3.30.3). Only miRNAs with FPKM > 5, P value < .05, and fold change > 1.5 were considered differentially expressed miRNAs (DE-miRNAs)

2.6. Prediction of miRNA target genes and function annotation

The potential target genes of sequenced miRNAs were predicted by MiRanda and RNAhybrid.[18] Gene function was annotated based on the Gene Ontology (GO) database. Functional enrichment was implemented and visualized using cluster Profiler4, ClueGO, and Metascape (https://metascape.org).

2.7. Identification of DEGs

The Zhan myeloma dataset[19] (http://lambertlab.uams.edu) is a microarray data of gene expression which included bone marrow plasma cells from 74 cases of NDMM, and 31 healthy donors. Limma package[20] (version 3.46.0) was used to identify differentially expressed genes (DEGs) between MMs and healthy donors. For DEGs, the P value was set at <.05.

2.8. Construction of the exosomal miRNA-mRNA network

Among the previously described DE-miRNAs, the top 6 hub exosomal miRNAs with high confidence were identified by plug-in CytoHubba of Cytoscape v3.7.2 using the MCC algorithm. Target genes of DE-miRNAs were selected according to the following criteria: (a) mRNA should be targeted by miRNAs; (b) the levels of mRNAs were negatively correlated with miRNA expression; (c) the target genes present differential expression in MM cells. The Metascape database was applied to assess the protein–protein interaction (PPI) network and functional modules. The top 40 genes with high confidence were identified as core target genes calculated by the PPI network with CytoHubba according to the degree score. Furthermore,

we also used Cytoscape to visualize the interactions between the hub miRNAs and target genes.

2.9. Establishment of a 13-core-gene signature

The effect of core genes on overall survival (OS) of MM patients was evaluated by univariate Cox regression. The least absolute shrinkage and selection operator (LASSO) Cox regression model was then used to narrow down the candidate genes and to develop the prognostic model. Multivariate Cox analysis was performed to obtain the risk score formula for hub genes. The prognostic risk score was calculated as follows: Risk score = exp(miRNA1) × β(miRNA1) + exp(miRNA2) × β(miRNA2) + …… + exp(miRNAn) × β (miRNAn) (where "exp" is the miRNA expression level and "β" is the regression coefficient obtained from the multivariate Cox analysis). Based on the above formula, the risk score of each patient was calculated. The "survival," "survminer," and "timeROC" R packages were employed to perform 1-, 3-, and 5-year receiver operating characteristic (ROC) curve analyses. In addition, the Kaplan–Meier method was used to calculate the OS rate for patients of the low-risk and high-risk groups, and the log-rank test was performed to compare survival differences between the two groups. Optimal cutoff points were calculated with R packages "survminer" using the maximally selected rank statistics.

2.10. Tumor cell characteristics in MM patients with diverse 13-core-gene signatures

MM patients in the GEO dataset GSE2658 cohort were stratified into 2 subgroups by the 13-core-gene signature according to the optimal cutoff point calculated with survminer. The DEGs between the low- and high-score groups were screened by limma package according to |log2FC| ≥ 1 and P value <.05. Gene set enrichment analysis (GSEA) between the 2 groups was performed using the Java implementation of GSEA software (version 4.0). The Broad Institute GSEA website (www.broad.mit.edu/gsea) provides detailed information on the computational method. The "gsva" package was used to conduct the single sample GSEA (ssGSEA) to calculate the scores of UAMS-70 genes and 56 drug-resistance genes. Statistical analyses of scores between the two groups used the unpaired Wilcoxon test.

2.11. Immune status analysis

The ESTIMATE immune scores[21] were used to analyze the infiltration levels of immune cells in MM patients with GSE136324.[22] The association between the gene signature and immune features was tested with Pearson correlation. The expression of HLA family genes was analyzed in different risk-group MM patients from GSE2658.

2.12. Statistical analysis

Data analyses were performed with R language and GraphPad Prism 8.0 Software. Statistical significance was set at $P < .05$. *$P < .05$, **$P < .01$, and ***$P < .001$.

3. RESULTS

3.1. The exosomal miRNA profile of MM patients by RNA sequencing

From peripheral blood samples collected from 9 healthy donors and 19 MM patients (Fig. 1A), exosomes from human serum were identified by their morphology, diameter, concentration, and the presence of exosome-enriched protein markers such as CD9, CD63, and TSG101. Electron microscopic images (Supplemental Fig. 1A, http://links.lww.com/BS/A58) showed that EVs were cup-shaped structures with a diameter of about 100 nm. Nanoparticle tracking analysis (Supplemental Fig. 1B, http://links.lww.com/BS/A58) revealed that the isolated EVs had a median diameter of 85.1 nm. Furthermore, these EVs were positive for CD9, CD63, and TSG101 proteins, but negative for calnexin (Supplemental Fig. 1C, http://links.lww.com/BS/A58), which is consistent with the standard for exosome isolation.[23]

According to small RNA data, a total of 2588 hsa-miRNAs were identified in the serum exosome samples of the 19 MM patients and 9 healthy donors. Through assessing the expression levels of serum exo-miRNAs in MM patients compared with healthy donors, we found 313 DE-miRNAs (|Log2FC|>1 and P value < .05). Among them, 158 were up-regulated, and 155 were down-regulated in MM patients. The volcano map showed the 313 DE-miRNAs (Fig. 1B). The top 10 up-regulated and down-regulated miRNAs are listed in Supplemental Fig. 1D, http://links.lww.com/BS/A58.

3.2. Target gene prediction and pathway involvement analysis

A total of 9564 target genes of the 313 differentially expressed miRNAs were predicted by MiRanda and RNAhybrid. The main biological processes, molecular function, and pathway analyses by GO analysis are summarized in Figure 1C, which shows these target genes were mainly involved in the proteasome-mediated ubiquitin-dependent protein catabolic process, regulation of protein stability, and regulation of DNA metabolic processes. To identify critical DE-miRNAs, Cytoscapev3.6.1 was used to map the miRNA-mRNA regulatory network of miRNA and its target genes, and CytoHubba was applied to screen the hub miRNAs. Of note, the top 6 hub miRNAs were identified according to the MCC score, including three up-regulated miRNAs: hsa-miR-4728-5p, miR-455-3p, and hsa-miR-6779-5p, as well as three down-regulated miRNAs: hsa-miR-124-3p, hsa-miR-615-3p, and hsa-miR-7106-5p (Fig. 1D).

3.3. Exosomal miRNA-mRNA regulatory network analysis

To elucidate the function of the exo-miRNAs, the miRNA-mRNA regulatory network was analyzed. The Zhan myeloma mRNA datasets containing "Multiple Myeloma versus Normal" in the Oncomine database included 74 MM patients and 31 normal individuals, and a total of 2463 DEGs were obtained (Supplemental Table 1, http://links.lww.com/BS/A59). Then, target genes of the 6 hub miRNAs mentioned above were predicted by MiRanda and RNAhybrid analysis (Supplemental Table 2, http://links.lww.com/BS/A59). One thousand four hundred eighty-two target genes of three up-regulated miRNAs (hsa-miR-4728-5p, miR-455-3p, and hsa-miR-6779-5p), and 2891 target genes of three down-regulated miRNAs (hsa-miR-124-3p, hsa-miR-615-3p, and hsa-miR-7106-5p) were identified. On account of the wide regulation of miRNA on mRNA expression, we focused on the target genes that met the following criteria: (a) mRNA should be targeted by miRNAs; (b) the levels of mRNA were negatively correlated with miRNA expression; (c) the target genes presented differential expression in MM cells according to the Zhan myeloma microarray data. Therefore, 513 genes (93 up-regulated and 420 down-regulated) were identified as the core mRNAs targeted by the 6 hub exo-miRNAs (Fig. 2A and Supplemental Table 3, http://links.lww.com/BS/A59). Taken together, these results identified promising miRNAs and their target genes for further analysis. The PPI network between these 513 core genes was constructed by STRING (Fig. 2B). Gene module analysis was used to further identify critical gene modules (Fig. 2C). According to the gene module score, we noted that mRNA splicing, cellular response to stress, and deubiquitination, which are involved in the pathogenesis of MM, were the top three modules of the core mRNAs

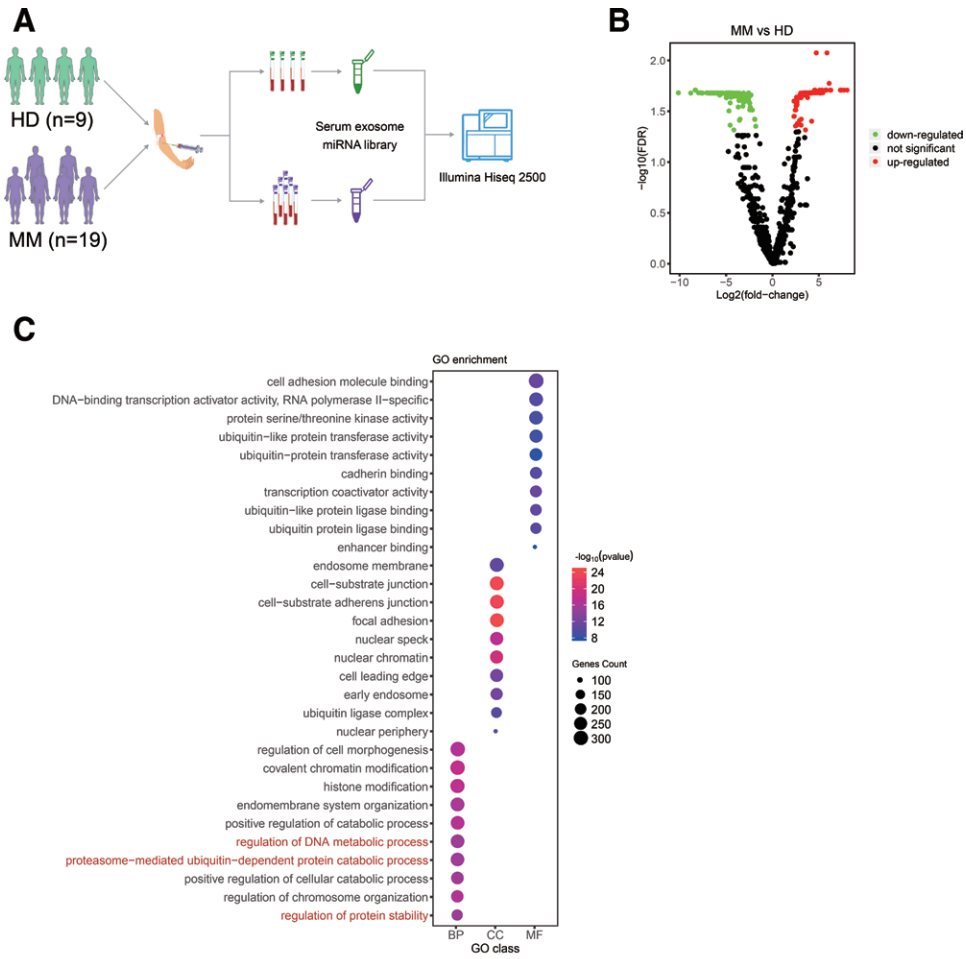

D

Rank	Name	Score	logFC	P-Value
1	hsa-miR-124-3p	1447	-4.15375	0.000663
2	hsa-miR-615-3p	893	-4.17493	0.01049
3	hsa-miR-4728-5p	838	3.237569	0.00696
4	hsa-miR-7106-5p	784	-6.17491	0.00029
4	hsa-miR-455-3p	784	2.365953	0.003709
6	hsa-miR-6779-5p	667	1.952113	0.010002

Figure 1. Distinct exosomal miRNA profiles in MM and healthy donors. (A) Serum exosomes from peripheral blood were collected from 9 healthy donors and 19 MM patients for miRNA sequencing. (B) Volcano plot illustrating miRNAs (DE-miRNAs) in serum exosomes differentially expressed between MM patients and healthy donors. (C) Bubble plot showing GO-enriched pathways of DE-miRNA target genes. (D) Table displaying top six hub DE-miRNAs calculated by the miRNA-mRNA regulatory network with CytoHubba. DE = differentially expressed, GO = gene ontology, MM = multiple myeloma.

targeted by hub exo-miRNAs (Fig. 2D). Genes in each module are listed in Supplemental Table 4, http://links.lww.com/BS/A59.

3.4. Functional analysis of core mRNAs targeted by hub exo-miRNAs

According to the PPI network of the 513 core genes targeted by exo-miRNAs, the CytoHubba analysis was further applied to screen pivotal genes among the network, and the top 40 target genes were defined by the degree method, including IL6, MDM2, PSMD2, and RPL23 (Supplemental Table 5, http://links.lww.com/BS/A59). Next, the miRNA-mRNA regulatory network of the 6 hub miRNAs and the 40 core target genes were analyzed by Cytoscape (v3.6.1, Fig. 3A). Pathway enrichment analysis by ClueGO indicated that the 40 core target genes were mainly involved in protein folding chaperoning, positive regulation of transcription of nucleolar large rRNA, negative regulation of proteolysis and positive regulation of miRNA metabolic process, as shown in Figure 3B. Of note, immune-related pathways were also significantly enriched, including cellular response to IL-4 and positive regulation of IL-8 production (orange and green, Fig. 3B).

3.5. Clinical significance of the 40 core target genes in MM

Next, we further analyzed the clinical significance of the core target genes in MM patients. The univariate analysis identified that 30 genes correlated with patient survival. Among them, 25 genes—examples included CCT5, CDKN2A, CDK4, CCT7,

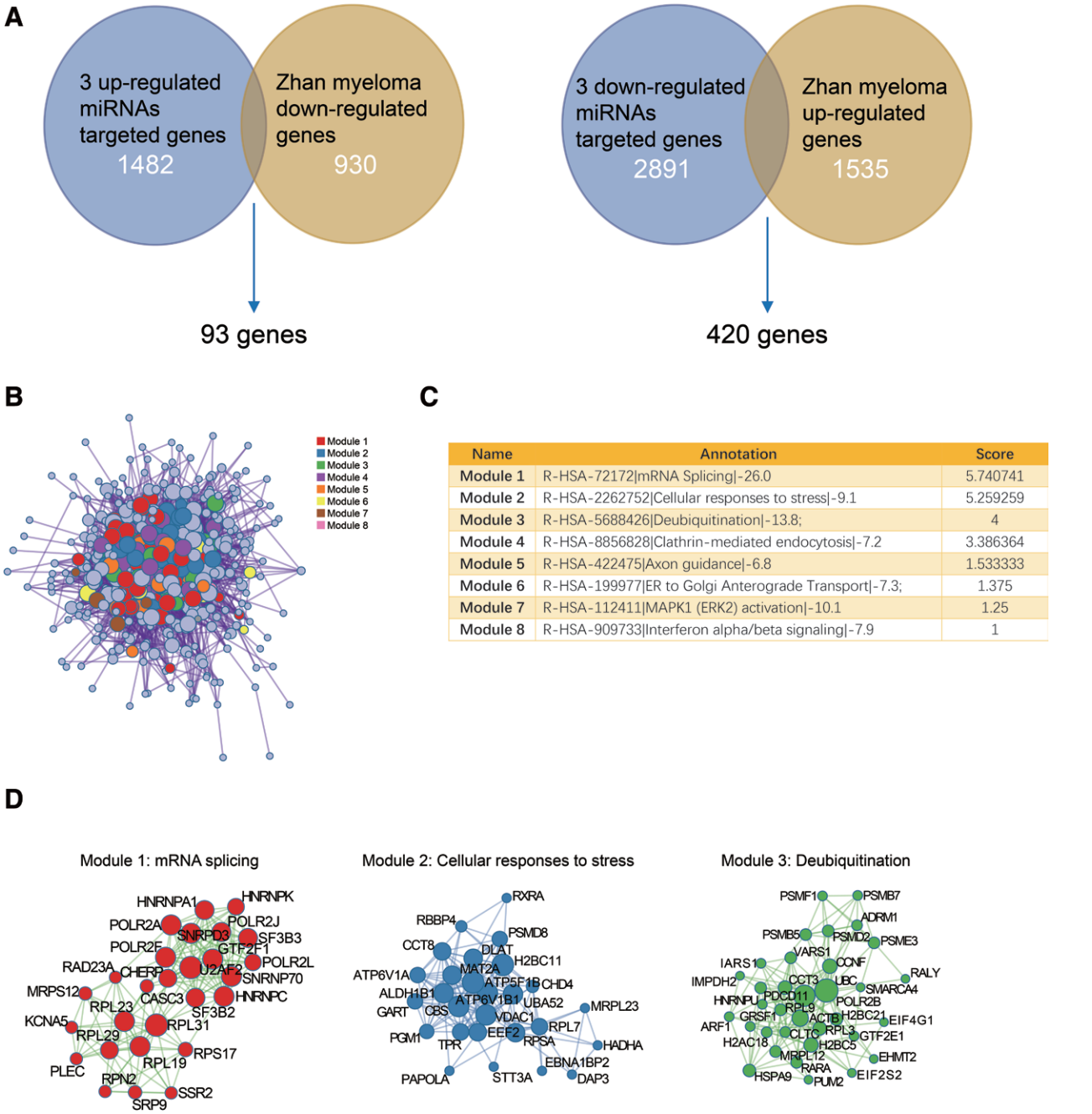

Name	Annotation	Score
Module 1	R-HSA-72172|mRNA Splicing|-26.0	5.740741
Module 2	R-HSA-2262752|Cellular responses to stress|-9.1	5.259259
Module 3	R-HSA-5688426|Deubiquitination|-13.8;	4
Module 4	R-HSA-8856828|Clathrin-mediated endocytosis|-7.2	3.386364
Module 5	R-HSA-422475|Axon guidance|-6.8	1.533333
Module 6	R-HSA-199977|ER to Golgi Anterograde Transport|-7.3;	1.375
Module 7	R-HSA-112411|MAPK1 (ERK2) activation|-10.1	1.25
Module 8	R-HSA-909733|Interferon alpha/beta signaling|-7.9	1

Figure 2. Functional modules of hub DE-miRNAs. (A) Venn plots showing the screening process of hub miRNAs and core target mRNAs. (B) PPI network of core target mRNAs with eight functional modules. (C) Table showing eight functional modules of core target mRNAs. (D) Interaction networks displaying detailed top three functional modules of core target mRNAs. DE = differentially expressed, PPI = protein–protein interaction.

HSPA9, CHD4, and HIST2HBE—were negatively correlated with patient survival. Five genes, RPL3, ACTB, EEF2, RPL23, and PIK3CA, were positively correlated with patient survival in GEO dataset GSE2658 (Fig. 4A). These survival-related genes were further investigated as to whether they could be used for prognostic stratification in patients. To avoid potential over-fitting, 13 core genes (which included CCT7, RPL23, CCT3, MARS, and PI3KCA) were optimized among 30 survival-related genes through LASSO Cox regression analysis, and a prognostic model based on them was developed (Fig. 4B and C). The risk score calculation formula was: risk score = (0.209*CCT7 exp.) + (−0.030*RPL23 exp.) + (0.019*CCT3 exp.) + (0.090*MARS exp.) + (−0.158*PIK3CA exp.) + (0.257*IL6 exp.) + (0.0015*CCT5 exp.) + (0.252*CDKN2A exp.) + (0.321*GART exp.) + (0.022*GAPDH exp.) (0.0567*HNRNPC exp.) + (−0.010*RPL3 exp.) + (0.176*MDM2 exp.). Time-dependent ROC analysis was applied to evaluate the sensitivity and specificity of the 13-core-gene signature model, and the area under the ROC curve (AUC) was 0.672 for 1-year, 0.728 for 3-year, and 0.744 for 5-year survival, respectively (Fig. 4D). The Kaplan–Meier survival analysis in two independent myeloma patient cohorts (GSE2658 and GSE136337) revealed that the OS was notably shorter in the high-score than in the low-score group (HR = 4.2, $P < .0001$; HR = 1.7, $P < .014$; Fig. 4E and F). Additionally, we validated the prognostic significance of 13 gene models in another four datasets, including two GFP datasets (GSE9782; GSE4452), one outside RNA-seq dataset (MMRF), and our center's own RNA-seq dataset. Kaplan–Meier survival analysis revealed that the OS was notably shorter in the high-score than in the low-score group (GSE9782: HR = 2.07,

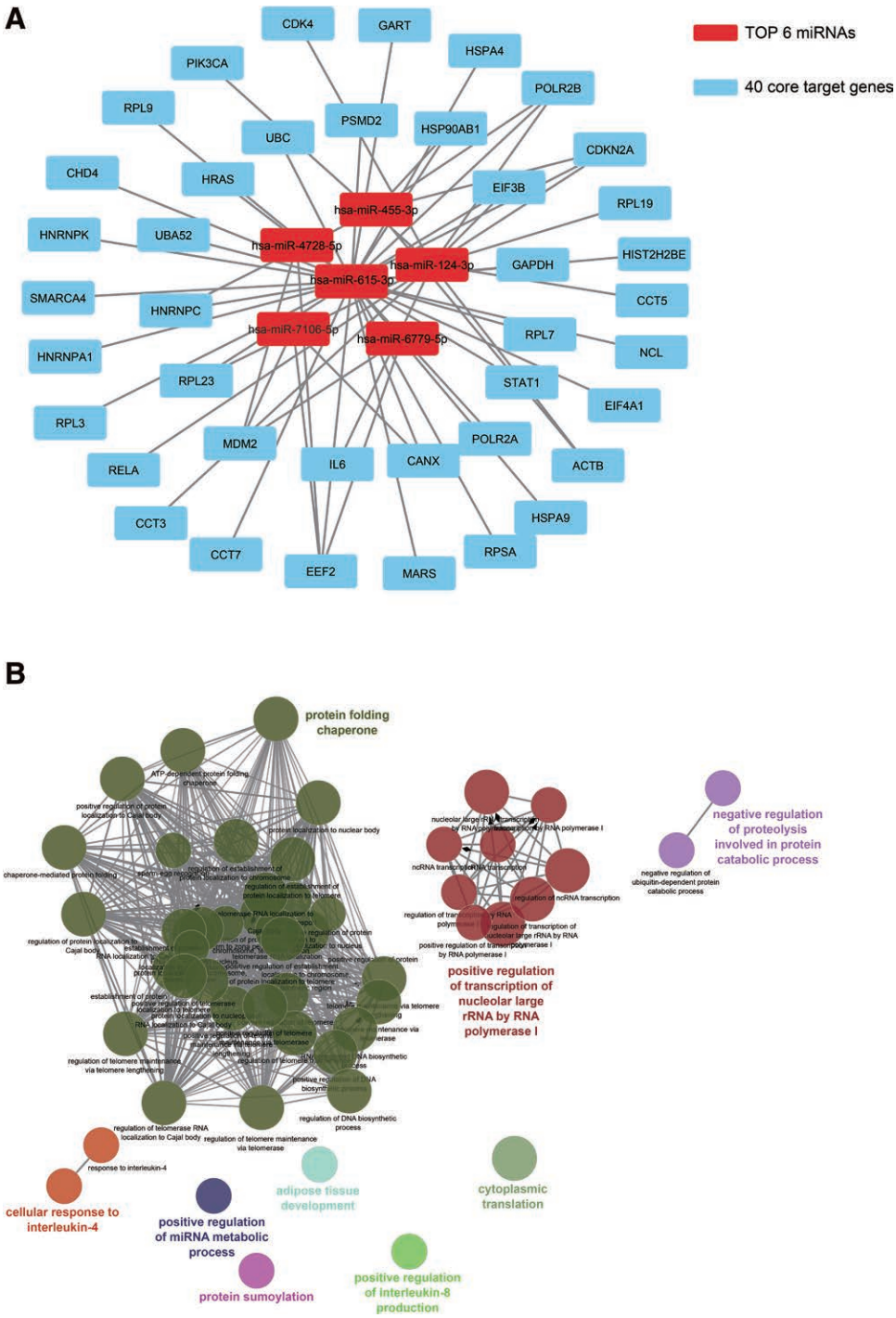

Figure 3. Exosomal hub miRNA-mRNA network in MM. (A) Regulatory network of 6 hub miRNAs and 40 core target genes. MiRNAs are labeled by red rectangles, while core genes are blue. (B) Network displaying enriched pathways identified by ClueGO of 40 core target genes. MM = multiple myeloma.

P = .0003; GSE4452: HR = 8.24, P < .0001; MMRF: HR = 2.07, P < .0001; Our center's RNA-seq: HR = 2.31, P < .0015; Supplemental Fig. 2A–D, http://links.lww.com/BS/A60).

These results showed that the 13-core-gene signature could be used to predict the OS of patients with MM.

3.6. Functional enrichment analysis of the 13 core genes

Owing to the prognostic stratification by the 13-core-gene signature identified above, 2 groups of MM patients with diverse outcomes were recognized. Between the 2 groups of patients, a total of 2144 up-regulated and 2694 down-regulated genes were identified in their myeloma cells (Fig. 5A). GSVA data showed significantly enriched pathways related to cell proliferation and protein homeostasis in the high-score group, including G2M checkpoint (NES = 2.38, P < .0001, FDR < 0.0001), E2F targets (NES = 2.35, P < .0001, FDR < 0.0001) and unfolded protein response (NES = 1.66, P = .04, FDR = 0.031). Interestingly, pathways related to metabolism were also up-regulated in high-score patients, including glycolysis (NES = 2.09, P < .0001, FDR = 0.001), fatty acid metabolism (NES = 1.90, P < .0001, FDR = 0.007), and oxidative phosphorylation (OXPHOS) (NES = 1.97, P = .002, FDR = 0.003). These findings indicated a relatively active metabolic status of

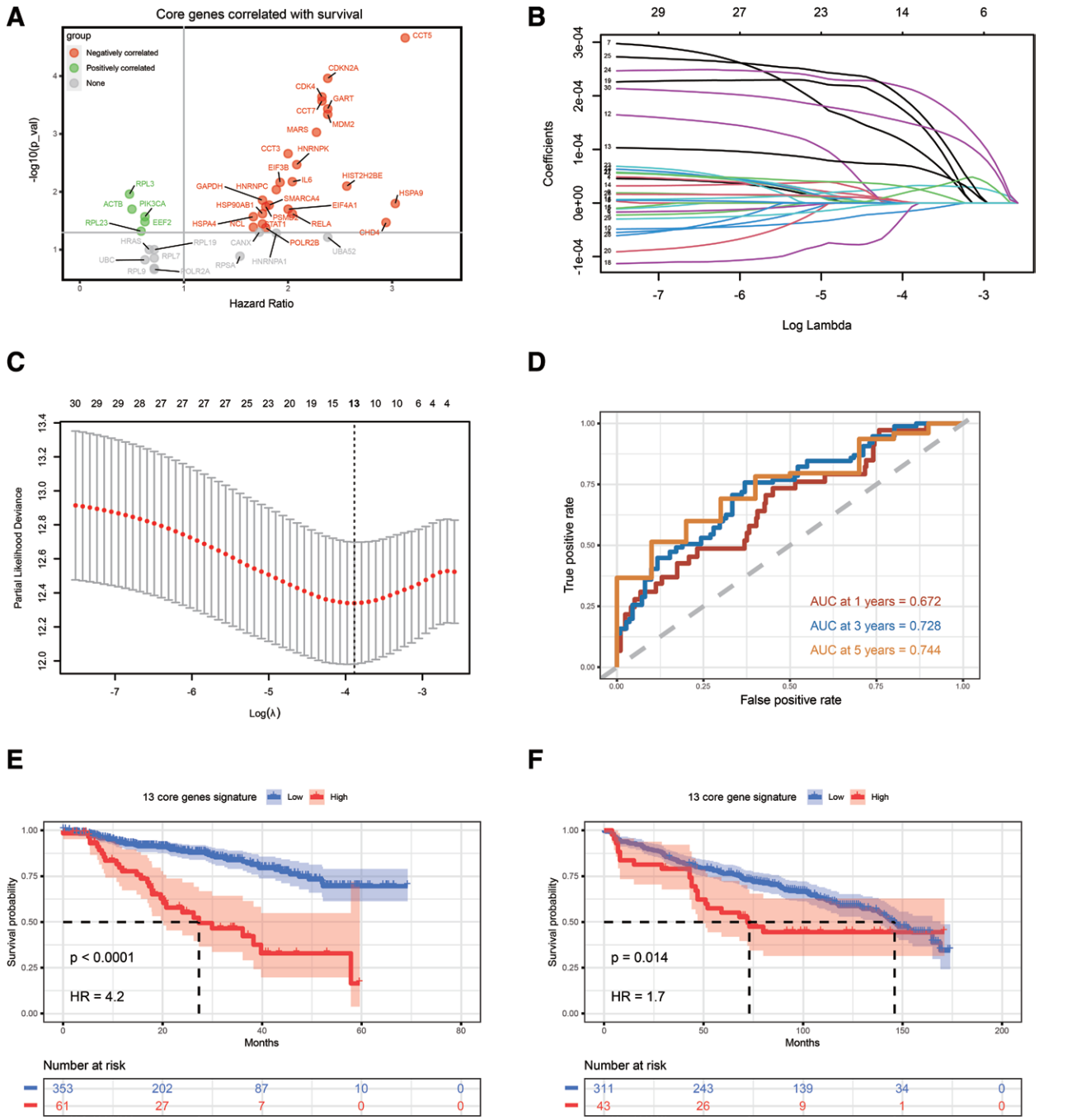

Figure 4. Construction of prognostic 13-core-gene signature based on core target genes. (A) Dot plot showing the relation of core target genes with MM patient OS. (B) LASSO coefficient profiles of the 30 risk factors. (C) 11 risk factors were selected using LASSO Cox regression analysis. The dotted vertical lines were drawn at the optimal scores by minimum criteria. (D) The ROC plot showing the accuracy of predicting 1-, 3-, and 5-year OS of MM patients by 13-core-gene signature. (E) Kaplan–Meier analysis of the 13-core-gene signature in MM patients from GSE2658. (F) Validation of the 13-core-gene signature in MM patients from GSE136324. LASSO = least absolute shrinkage and selection operator, MM = multiple myeloma, OS = overall survival, ROC = receiver operating characteristic.

tumor cells in these high-score patients (Fig. 5B). Zhan et al previously reported the molecular classification of myeloma UAMS-7, which divided patients into seven subgroups: CD1, CD2, HY, LB, MF, MS, and PR.[24] Our study indicated that the patients identified in our high-score group were consistently distributed in the high-risk subgroups of UAMS-7, including MF, MS, and PR (Fig. 5C). Previous studies demonstrated a 70-high-risk gene set (UAMS-70) and a 56-drug-resistance gene set were associated with poorer outcomes in MM.[25,26] Here, we examined the expression of these malignant genes within two groups of patients with diverse 13-core-gene signatures. The patients in the high-core group displayed higher 70 high-risk gene set (UAMS-70) and 56 drug-resistance gene set expression. These findings supported the conclusion that the patients with high scores of the 13-core-gene signature had poorer outcomes (Fig. 5D and E).

From previous studies, we know that reversible epigenetic RNA processes, such as m6A, m5C, m1A, and m7G modification, play prominent roles in various biological processes, including myeloma occurrence and immune regulation in

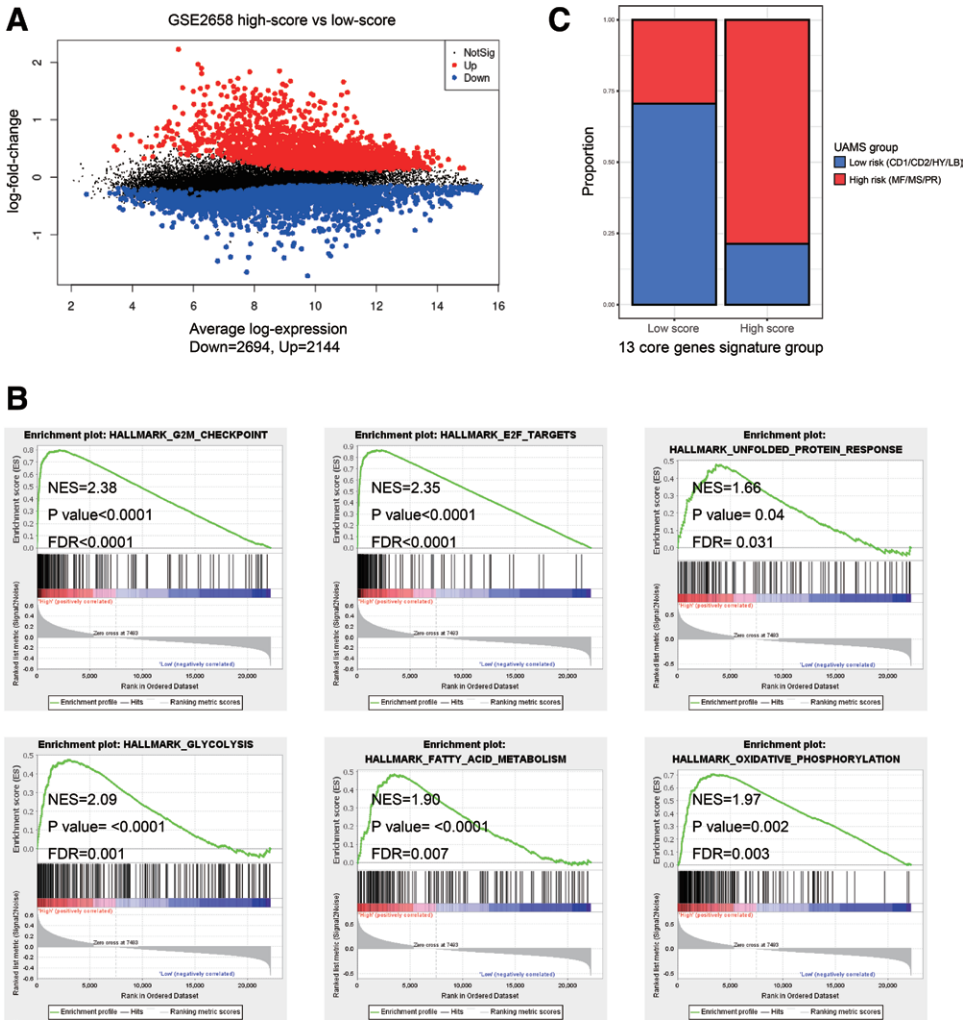

Figure 5. Difference between two groups of MM patients distinguished by 13-core-gene signature. (A) Volcano plot displaying DEGs between MM patients in different groups identified by 13-core-gene signature. (B) GSEA plots illustrating significantly enriched pathways in high-score patients identified by 13-core-gene signature. (C) Stacked bar plot showing the distribution of UAMS-7 groups for MM patients in different groups identified by 13-core-gene signature. (D) Heatmap showing the expression of 70 high-risk genes in different groups of MM patients identified by the 13-core-gene signature (left). Boxplot displaying 70 high-risk gene scores calculated by GSVA in different groups of MM patients (right). (E) Heatmap (left) and boxplot (right) showing the expression of 56 drug resistance-related genes in different groups of MM patients distinguished by 13-core-gene signature. (F) Boxplots showing different profiles of m6A, m5C, m1A and m7G modification in different groups of MM patients from GSE2658. DEG = differential expression gene, GSVA = gene set variation analysis, MM = multiple myeloma.

hematological malignancy.[27,28] Of note, we found that the level of m6A modification genes (ELAVL1, HNRNPA2B1, HNRNPC, LRPPRC, RBM15, YTHDC1, and YTHDF2), m5C modification genes (ALYREF, NSUN2, and NSUN3), m1A modification genes (ALKBH3 and YTHDF2) and the m7G modification gene, METTL1, were significantly increased in patients with high 13-core-gene signature scores, while the expressions of m6A modification gene, YTHDC1, and m5C modification genes, NSUN4 and NSUN6, were significantly increased in the low-score group (Fig. 5F).

3.7. Analysis of immune status

Immune escape is a hallmark of malignancies, including MM. Given that immune-related terms were significantly enriched in the 40 core target genes identified above, we speculated that the 13-core-gene signature model could reflect the immune state of myeloma patients. Here, the tumor immune microenvironment was assessed using the immune score, ESTIMATE score, and stromal score. As Figure 6A shows, these immune scores were negatively correlated with the 13-core-gene signature score, indicating a stronger immune cell infiltration level in low-score than in high-score patients. In addition, tumor purity score was positively correlated with the 13-core-gene signature score, suggesting a higher tumor cell burden in high-score patients (Fig. 6B). The HLA genes that are found on the surfaces of tumor cells participate in antigen processing and presentation in antitumor immunity. Our data showed that the HLA family genes, including HLA-A, HLA-B, HLA-C, HLA-D, HLA-E, HLA-F, HLA-G, HLA-DRB6, HLA-DQB1, HLA-DQB2, HLA-DPB1, HLA-DPB2, HLA-DPA2, HLA-DOB, and HLA-DMB, showed a comprehensively significant decrease in MM cells of high-score group patients (Fig. 6C). These findings indicated that the 13-core-gene signature model was correlated with aberrant immune status in MM patients.

4. DISCUSSION

Circulating miRNAs are generated by two main mechanisms: cell death by apoptosis or necrosis, leading to the release of miRNAs bound to Argonaute (AGO) proteins, and an active process by secretion of exosomes containing miRNAs.[29] Thus, exosomal

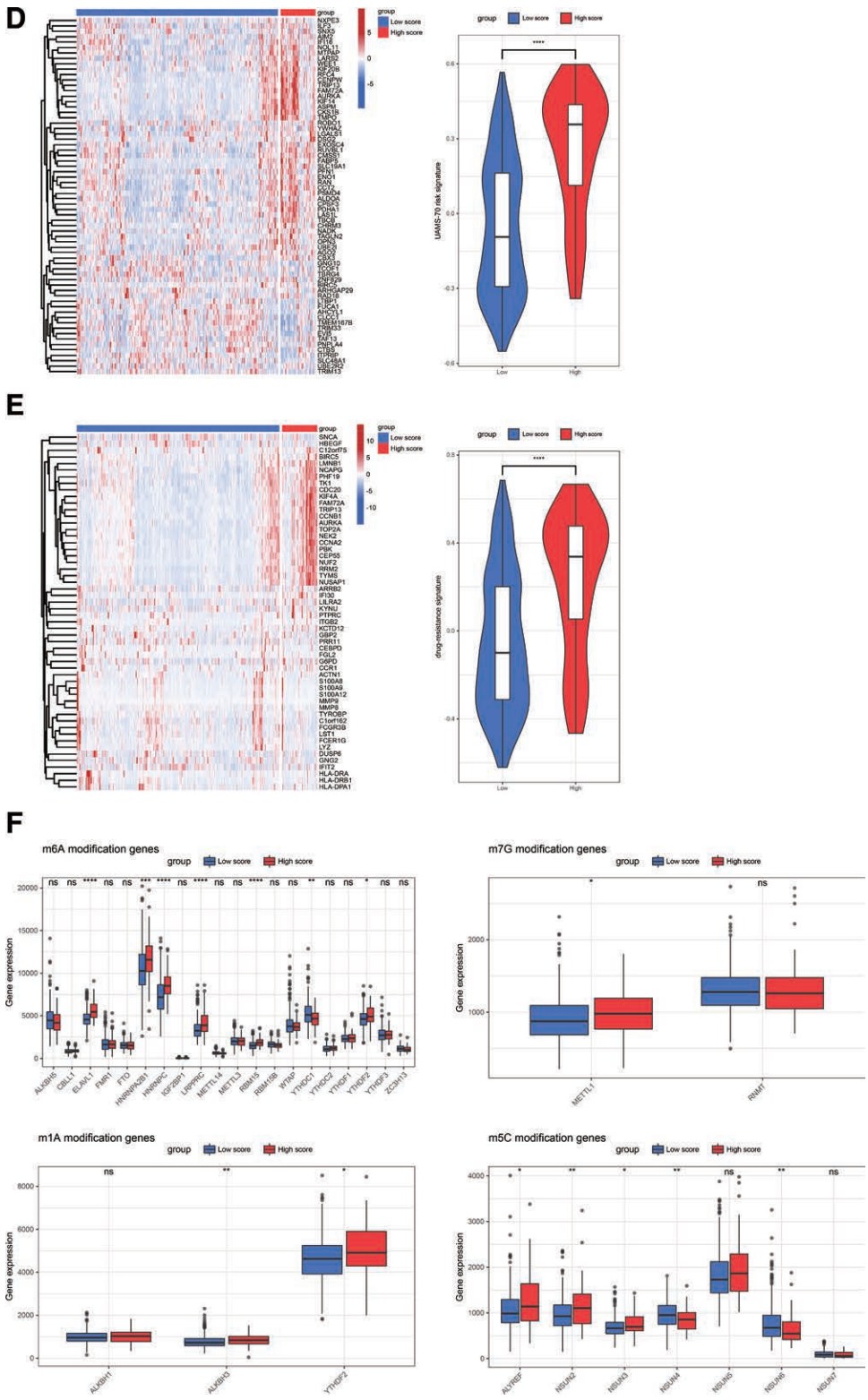

Figure 5. Continued

miRNAs could represent a more specific molecular biomarker than cell-free miRNAs. Currently, there is a trend toward using serum exosomal cargo, including miRNAs, as promising noninvasive biomarkers for prognosis prediction in numerous diseases as a result of their accessibility and the stabilized level for detection.[30,31] In addition, several studies have demonstrated that miRNAs (exo-miRNAs) play critical roles in communication between cells, especially in the pathogenesis of malignancies.[11,32] In our study, 313 serum exo-miRNAs differentially expressed between MM patients and healthy donors were clarified. The number of DE-miRNAs identified in our study was far more than reported by Manier et al.[10] GO analysis of target genes of differential miRNAs showed that these target genes are mainly involved in critical biological processes related to MM pathogenesis such as

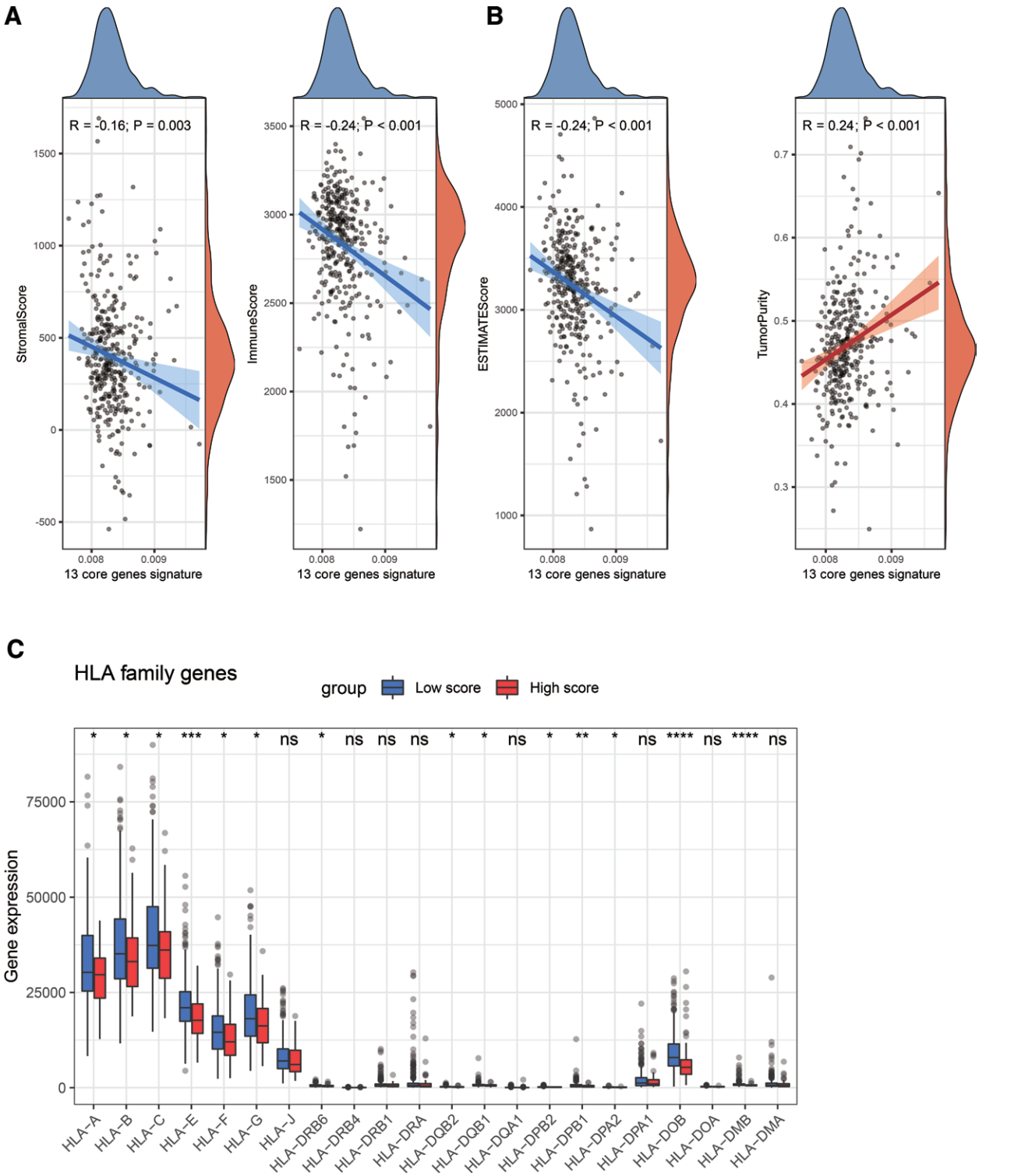

Figure 6. Correlation between 13-core-gene signature and immune status. (A) Fitted curves showing Pearson's correlation between 13-core-gene scores and the stromal scores, the immune score and the ESTIMATE score in MM patients from GSE136324. (B) Fitted curves showing Pearson's correlation between 13-core-gene scores and the tumor infiltration in MM patients from GSE136324. (C) Boxplots showing different expressions of HLA family genes in different groups of MM patients from GSE2658. MM = multiple myeloma.

the proteasome-mediated ubiquitin-dependent protein catabolic process, and regulation of protein stability, indicating the indispensable roles of these miRNAs in MM pathogenesis. Because of the limited scale of patients in our study, the levels of these exo-miRNAs, especially the top six hub exo-miRNAs, need to be further confirmed on a larger scale.

MiRNAs carried by the exosomes released from various cell types including MM cells are involved in multiple types of cell–cell interactions. In addition, multiple miRNAs have been shown to modulate the expression of genes critical for MM pathogenesis. For instance, miR-15a and miR-16 were down-regulated by the IL-6 secretion from bone marrow stem cells (BMSC)

and promoted drug resistance in MM cells.[32] Furthermore, loss of miR-29 family members increases proteasome activator complex subunit 4 (PSME4) expression and PSME4 levels to elevate proteasome activity and render cells therapeutically resistant to proteasome inhibitors,[33] miR-21 inhibits STAT3, which mediates RANKL gene activation. Inhibition of miR-21 restores the RANKL/osteoprotegerin ratio in MM-derived BMSCs and impairs the resorbing activity of mature osteoclasts, which contributes to myeloma bone disease.[34] According to the literature, the top six hub miRNAs observed in our study have been reported to play important roles in the occurrence and progression of malignancies, including MM. Liu et al reported that miR-615 was a tumor suppressor by targeting protein kinase C beta (PRKCB) and exerting antimyeloma activity, and the miR-615-3p/PRKCB axis could regulate the sensitivity of MM cells to proteasome inhibitor.[35] Chen et al reported that miR-124 was down-regulated in MM cells and caused overexpression of the target gene growth factor receptor-bound protein 2, which promoted MM cell survival and growth.[36] Furthermore, these miRNAs are also involved in many kinds of solid tumors. MiR-455 was reported to function as an oncomiR in esophageal squamous cell carcinoma progression through activating the Wnt/β-catenin and transforming growth factor-β/Smad pathways.[37] MiR-4728 was reported to be an important tumor suppressor miRNA that controls MAPK signaling through targeting mammalian STE20-like protein kinase 4 (MST4), revealing the significance of miR-4728 as a potential prognostic factor and target for therapeutic intervention in cancer.[38]

The ubiquitin-proteasome system is known to be critical for MM cell survival, which maintains the protein homeostasis of MM cells.[39] The dynamic process of ubiquitination and deubiquitination efficiently modulates protein stabilization and degradation.[40,41] As expected, we found that the target genes of the top six hub miRNAs were mainly enriched in the deubiquitination process signal pathway, which indicates the reliability of the results demonstrated in this study. Moreover, we found that target genes were enriched in the mRNA splicing pathways. Alternative splicing allows pre-mRNA to be processed into different mature mRNAs, thereby expanding the cellular proteome.[42] Recent studies highlighted that splicing process alterations have prognostic value and act as a hallmark of cancer progression.[43,44] Splicing alterations are often linked to the frequent occurrence of mutations in genes encoding either core components or regulators of the splicing machinery. Recent reports indicate that splicing machinery is markedly de-regulated in MM and represents a biomarker of disease aggressiveness.[45] Our results suggest that the top six hub exosomal differential miRNA target genes include those encoding either core components or regulators of the splicing machinery like SF3B2, SF3B3, and U2AF2, this suggests that tumor cells might alter the expression level of genes encoding splicing machinery by secreting exosomal miRNA, thereby altering the patterns of alternative mRNA splicing. Michael et al reported that high numbers of novel splice loci were associated with adverse survival of MM patients, and the enumeration of patterns of alternative splicing has the potential to refine MM classification and assist in the risk stratification of patients,[46] which supports our findings.

Additionally, our data identified that 13 core genes among 40 core target genes could be efficiently applied to predicting clinical outcomes in myeloma. The risk model had AUCs of 0.672, 0.728, and 0.744 for predicting 1-, 3-, and 5-year OS, respectively, indicating high accuracy and reliability. Moreover, OS was significantly lower in the high-score than in the low-score group, which confirmed its predictive efficiency. Metabolism-related pathways, including glycolysis, fatty acid metabolism, and oxidative phosphorylation (OXPHOS), were significantly up-regulated in the high-score group. Previous research demonstrated that increased fatty acid synthesis, glycolysis, and OXPHOS are necessary for ensuring that enough energy is available for rapid cell proliferation in MM.[47] Our study further validated that aberrant metabolic status may affect patient clinical outcomes. Moreover, the high-score patients identified by the 13-core-gene signature displayed higher 70 high-risk gene set (UAMS-70) scores, as well as the 56 drug-resistance genes set score, which might partly explain their inferior outcomes. RNA modification, including m6A, m5C, m1A, and m7G, is a reversible epigenetic RNA process, that is required for cancer-cell survival, and targeting this pathway has been proposed as a new therapeutic strategy.[28,48] In our study, the expression of various modification genes was analyzed within the high- and low-score groups, and aberrant expression status of m6A, m5C, m1A, and m7G RNA methylation regulators in MM was identified. Previous research reported that four m6A regulators (ZC3H13, HNRNPA2B1, HNRNPC, and ZC3H13) based on prognostic risk score can accurately predict the survival of MM patients, indicating the indispensable role of RNA methylation in MM progression.[28] Our results also showed that HNRNPA2B1 and HNRNPC were up-regulated in high-score MM patients. The biological functions of several RNA modification genes in MM have been investigated by other researchers. HNRNPA2B1, an m6A reader, was elevated in MM patients and negatively correlated with favorable prognosis; it potentially acts as a therapeutic target of MM.[49] YTHDF2, another m6A reader, was also increased in MM patients and associated with poor outcomes. YTHDF2 was reported to bind to the m6A modification site of STAT5A to promote its mRNA degradation, while STAT5A suppressed MM cell proliferation by occupying the transcription site of MAP2K2 to decrease ERK phosphorylation. The YTHDF2/STAT5A/MAP2K2/p-ERK axis plays a key role in MM proliferation, and targeting YTHDF2 may be a promising therapeutic strategy.[50] Consistently, the 2 genes were up-regulated in our patients in the high-score group. These results further support the value of our risk score model and imply the potentially significant roles of RNA modification-related genes in MM.

The evolution of MM depends on an immunosuppressive milieu that fosters immune escape and tumor progression.[51] In the present study, a striking finding was that these 40 core target genes were significantly enriched in the cellular response to interleukin-4 and interleukin-8 pathways related to tumor immunity, providing an insight that MM cells may regulate a variety of immune cellular components in the bone marrow microenvironment through exosomes carrying miRNAs; this partly explains the suppressive immune state in the bone marrow. Our results indeed suggest that the 13-core-gene signature model based on the 40 core target genes was highly correlated with the status of the immune microenvironment, and patients in the low-score group had higher infiltration levels of immune cells. Furthermore, patients in the high-risk group displayed lower HLA family gene expression. Tumors have developed different strategies to evade immune surveillance, for example altering the expression of classical and nonclassical HLA molecules.[52–54] Based on our results, we hypothesize that the exosomal miRNAs could regulate the expression of HLA molecules of MM cells, and affect the infiltration of immune cells in the bone marrow microenvironment. Among the top six hub miRNAs, miR-124 has been reported to be a critical modulator of tumor immunity by directly targeting signal transducer and activator of transcription 3 (STAT3), a key component mediating immunosuppression in the tumor microenvironment.[55] A recent study reported a therapeutic approach that uses lipid nanoparticles to deliver miR-124, which targets STAT3, to very high levels in the immune compartment in vivo. This therapeutic method stimulated antitumor immune responses without significant toxicity, significantly prolonged survival in murine intracerebral glioma models, and induced immunological memory that

is protective of tumor rechallenge.[56] Our results suggest that miR-124 was down-regulated in MM serum exosomes, and it showed the highest CytoHubba score, indicating its critical role in MM pathology. However, further study is required to understand the overwhelmingly complex immune regulation network in the bone marrow microenvironment of myeloma mediated by exosome miRNA and their target genes, which might provide promising therapeutic targets.

5. CONCLUSION

In the present study, the expression profile of exo-miRNAs in the serum of MM patients has been evaluated. Through presenting a bioinformatics analysis of exo-miRNAs and their target genes, we identified 6 hub miRNAs and 40 core target genes, which provide potential therapeutic targets and a deeper understanding of the pathogenesis of MM. A 13-core-gene-based prognostic risk score was constructed, which can assist in accurately predicting the survival of MM patients. In addition, the risk score is closely associated with the aberrant immune infiltration level, which complements current prediction models.

ACKNOWLEDGMENTS

This work was supported by the National Natural Science Foundation of China (82170194, 81920108006, 82270175), and the CAMS Innovation Fund for Medical Sciences (CIFMS 2021-I2M-1-040, CIFMS 2022-I2M-022).

We express thanks for the information from the GEO dataset (GSE2658, GSE4452, GSE9782, GSE136324, and GSE136337) and MMRF-CoMMpass dataset.

AUTHOR CONTRIBUTIONS

Conception and design of the analysis: M.H., L.Q. Collection and assembly of data: T.F., H.S., Z.Y., LT.L., XY.S., LX.G., GQ.Z., Y.H., PX.T., ZS.X., SY.X., TY.W., SH.Y., G.A., Y.X. Data analysis and interpretation: T.F., H.S. Final approval of the manuscript: L.Q., M.H.

REFERENCES

[1] Kumar SK, Rajkumar V, Kyle RA, et al. Multiple myeloma. *Nat Rev Dis Primers* 2017;3:17046.
[2] García-Ortiz A, Rodríguez-García Y, Encinas J, et al. The role of tumor microenvironment in multiple myeloma development and progression. *Cancers (Basel)* 2021;13(2):217.
[3] Liu L, Yu Z, Cheng H, et al. Multiple myeloma hinders erythropoiesis and causes anaemia owing to high levels of CCL3 in the bone marrow microenvironment. *Sci Rep* 2020;10(1):20508.
[4] Hao M, Franqui-Machin R, Xu H, et al. NEK2 induces osteoclast differentiation and bone destruction via heparanase in multiple myeloma. *Leukemia* 2017;31(7):1648–1650.
[5] Théry C, Ostrowski M, Segura E. Membrane vesicles as conveyors of immune responses. *Nat Rev Immunol* 2009;9(8):581–593.
[6] Tkach M, Théry C. Communication by extracellular vesicles: where we are and where we need to go. *Cell* 2016;164(6):1226–1232.
[7] Yáñez-Mó M, Siljander PR, Andreu Z, et al. Biological properties of extracellular vesicles and their physiological functions. *J Extracell Vesicles* 2015;4:27066.
[8] Yu T, Du C, Ma X, et al. Polycomb-like protein 3 induces proliferation and drug resistance in multiple myeloma and is regulated by miRNA-15a. *Mol Cancer Res* 2020;18(7):1063–1073.
[9] Schickel R, Boyerinas B, Park SM, Peter ME. MicroRNAs: key players in the immune system, differentiation, tumorigenesis and cell death. *Oncogene* 2008;27(45):5959–5974.
[10] Manier S, Liu CJ, Avet-Loiseau H, et al. Prognostic role of circulating exosomal miRNAs in multiple myeloma. *Blood* 2017;129(17):2429–2436.
[11] Zhang L, Pan L, Xiang B, et al. Potential role of exosome-associated microRNA panels and in vivo environment to predict drug resistance for patients with multiple myeloma. *Oncotarget* 2016;7(21):30876–30891.
[12] Chen T, Moscvin M, Bianchi G. Exosomes in the pathogenesis and treatment of multiple myeloma in the context of the bone marrow microenvironment. *Front Oncol* 2020;10:608815.
[13] Boyiadzis M, Whiteside TL. The emerging roles of tumor-derived exosomes in hematological malignancies. *Leukemia* 2017;31(6):1259–1268.
[14] Yamamoto T, Kosaka N, Hattori Y, Ochiya T. A challenge to aging society by microRNA in extracellular vesicles: microRNA in extracellular vesicles as promising biomarkers and novel therapeutic targets in multiple myeloma. *J Clin Med* 2018;7(3):55.
[15] Langmead B, Trapnell C, Pop M, Salzberg SL. Ultrafast and memory-efficient alignment of short DNA sequences to the human genome. *Genome Biol* 2009;10(3):R25.
[16] Friedländer MR, Mackowiak SD, Li N, Chen W, Rajewsky N. miRDeep2 accurately identifies known and hundreds of novel microRNA genes in seven animal clades. *Nucleic Acids Res* 2012;40(1):37–52.
[17] Robinson MD, McCarthy DJ, Smyth GK. edgeR: a Bioconductor package for differential expression analysis of digital gene expression data. *Bioinformatics* 2010;26(1):139–140.
[18] Betel D, Wilson M, Gabow A, Marks DS, Sander C. The microRNA.org resource: targets and expression. *Nucleic Acids Res* 2008;36(Database issue):D149–D153.
[19] Zhan F, Hardin J, Kordsmeier B, et al. Global gene expression profiling of multiple myeloma, monoclonal gammopathy of undetermined significance, and normal bone marrow plasma cells. *Blood* 2002;99(5):1745–1757.
[20] Ritchie ME, Phipson B, Wu D, et al. limma powers differential expression analyses for RNA-sequencing and microarray studies. *Nucleic Acids Res* 2015;43(7):e47.
[21] Yoshihara K, Shahmoradgoli M, Martínez E, et al. Inferring tumour purity and stromal and immune cell admixture from expression data. *Nat Commun* 2013;4:2612.
[22] Danziger SA, McConnell M, Gockley J, et al. Bone marrow microenvironments that contribute to patient outcomes in newly diagnosed multiple myeloma: a cohort study of patients in the Total Therapy clinical trials. *PLoS Med* 2020;17(11):e1003323.
[23] van Niel G, D'Angelo G, Raposo G. Shedding light on the cell biology of extracellular vesicles. *Nat Rev Mol Cell Biol* 2018;19(4):213–228.
[24] Zhan F, Huang Y, Colla S, et al. The molecular classification of multiple myeloma. *Blood* 2006;108(6):2020–2028.
[25] Shaughnessy JD, Jr., Zhan F, Burington BE, et al. A validated gene expression model of high-risk multiple myeloma is defined by deregulated expression of genes mapping to chromosome 1. *Blood* 2007;109(6):2276–2284.
[26] Zhou W, Yang Y, Xia J, et al. NEK2 induces drug resistance mainly through activation of efflux drug pumps and is associated with poor prognosis in myeloma and other cancers. *Cancer Cell* 2013;23(1):48–62.
[27] Zhao Y, Peng H. The role of N(6)-methyladenosine (m(6)A) methylation modifications in hematological malignancies. *Cancers* 2022;14(2):332.
[28] Liu R, Shen Y, Hu J, et al. Comprehensive analysis of m6A RNA methylation regulators in the prognosis and immune microenvironment of multiple myeloma. *Front Oncol* 2021;11:731957.
[29] Cortez MA, Bueso-Ramos C, Ferdin J, Lopez-Berestein G, Sood AK, Calin GA. MicroRNAs in body fluids--the mix of hormones and biomarkers. *Nat Rev Clin Oncol* 2011;8(8):467–477.
[30] Mitchell PS, Parkin RK, Kroh EM, et al. Circulating microRNAs as stable blood-based markers for cancer detection. *Proc Natl Acad Sci USA* 2008;105(30):10513–10518.
[31] Watson CN, Belli A, Di Pietro V. Small non-coding RNAs: new class of biomarkers and potential therapeutic targets in neurodegenerative disease. *Front Genet* 2019;10:364.
[32] Hao M, Zhang L, An G, et al. Suppressing miRNA-15a/-16 expression by interleukin-6 enhances drug-resistance in myeloma cells. *J Hematol Oncol* 2011;4:37.
[33] Jagannathan S, Vad N, Vallabhapurapu S, Vallabhapurapu S, Anderson KC, Driscoll JJ. MiR-29b replacement inhibits proteasomes and disrupts aggresome+autophagosome formation to enhance the antimyeloma benefit of bortezomib. *Leukemia* 2015;29(3):727–738.
[34] Pitari MR, Rossi M, Amodio N, et al. Inhibition of miR-21 restores RANKL/OPG ratio in multiple myeloma-derived bone marrow stromal cells and impairs the resorbing activity of mature osteoclasts. *Oncotarget* 2015;6(29):27343–27358.
[35] Liu J, Du F, Chen C, et al. CircRNA ITCH increases bortezomib sensitivity through regulating the miR-615-3p/PRKCD axis in multiple myeloma. *Life Sci* 2020;262:118506.

[36] Chen X, Liu Y, Yang Z, Zhang J, Chen S, Cheng J. LINC01234 promotes multiple myeloma progression by regulating miR-124-3p/GRB2 axis. *Am J Transl Res* 2019;11(10):6600–6618.
[37] Liu A, Zhu J, Wu G, et al. Antagonizing miR-455-3p inhibits chemoresistance and aggressiveness in esophageal squamous cell carcinoma. *Mol Cancer* 2017;16(1):106.
[38] Schmitt DC, Madeira da Silva L, Zhang W, et al. ErbB2-intronic microRNA-4728: a novel tumor suppressor and antagonist of oncogenic MAPK signaling. *Cell Death Dis* 2015;6(5):e1742.
[39] Saavedra-García P, Martini F, Auner HW. Proteasome inhibition in multiple myeloma: lessons for other cancers. *Am J Physiol Cell Physiol* 2020;318(3):C451–C462.
[40] Mofers A, Pellegrini P, Linder S, D'Arcy P. Proteasome-associated deubiquitinases and cancer. *Cancer Metastasis Rev* 2017;36(4):635–653.
[41] Yu Z, Wei X, Liu L, et al. Indirubin-3'-monoxime acts as proteasome inhibitor: therapeutic application in multiple myeloma. *EBioMedicine* 2022;78:103950.
[42] Lee Y, Rio DC. Mechanisms and regulation of alternative pre-mRNA splicing. *Annu Rev Biochem* 2015;84:291–323.
[43] Lee SC, Abdel-Wahab O. Therapeutic targeting of splicing in cancer. *Nat Med* 2016;22(9):976–986.
[44] Bonnal SC, López-Oreja I, Valcárcel J. Roles and mechanisms of alternative splicing in cancer - implications for care. *Nat Rev Clin Oncol* 2020;17(8):457–474.
[45] Soncini D, Martinuzzi C, Becherini P, et al. Apoptosis reprogramming triggered by splicing inhibitors sensitizes multiple myeloma cells to Venetoclax treatment. *Haematologica* 2022;107(6):1410–1426.
[46] Bauer MA, Ashby C, Wardell C, et al. Differential RNA splicing as a potentially important driver mechanism in multiple myeloma. *Haematologica* 2021;106(3):736–745.
[47] Gavriatopoulou M, Paschou SA, Ntanasis-Stathopoulos I, Dimopoulos MA. Metabolic disorders in multiple myeloma. *Int J Mol Sci* 2021;22(21):11430.
[48] Barbieri I, Kouzarides T. Role of RNA modifications in cancer. *Nat Rev Cancer* 2020;20(6):303–322.
[49] Jiang F, Tang X, Tang C, et al. HNRNPA2B1 promotes multiple myeloma progression by increasing AKT3 expression via m6A-dependent stabilization of ILF3 mRNA. *J Hematol Oncol* 2021;14(1):54.
[50] Hua Z, Wei R, Guo M, et al. YTHDF2 promotes multiple myeloma cell proliferation via STAT5A/MAP2K2/p-ERK axis. *Oncogene* 2022;41(10):1482–1491.
[51] Kawano Y, Moschetta M, Manier S, et al. Targeting the bone marrow microenvironment in multiple myeloma. *Immunol Rev* 2015;263(1):160–172.
[52] Leone P, Shin EC, Perosa F, Vacca A, Dammacco F, Racanelli V. MHC class I antigen processing and presenting machinery: organization, function, and defects in tumor cells. *J Natl Cancer Inst* 2013;105(16):1172–1187.
[53] Seliger B. The link between MHC class I abnormalities of tumors, oncogenes, tumor suppressor genes, and transcription factors. *J Immunotoxicol* 2014;11(4):308–310.
[54] Thuring C, Follin E, Geironson L, et al. HLA class I is most tightly linked to levels of tapasin compared with other antigen-processing proteins in glioblastoma. *Br J Cancer* 2015;113(6):952–962.
[55] Cao Q, Li YY, He WF, et al. Interplay between microRNAs and the STAT3 signaling pathway in human cancers. *Physiol Genomics* 2013;45(24):1206–1214.
[56] Yaghi NK, Wei J, Hashimoto Y, et al. Immune modulatory nanoparticle therapeutics for intracerebral glioma. *Neuro Oncol* 2017;19(3):372–382.